

Supplementary Information for

Iodous acid-a more efficient nucleation precursor than iodic acid

Shaobing Zhang,^{‡a} Shuning Li,^{‡ab} An Ning,^a Ling Liu^{*a} and Xiuhui Zhang^{*a}

^a Key Laboratory of Cluster Science, Ministry of Education of China, School of Chemistry and
Chemical Engineering, Beijing Institute of Technology, Beijing, 100081, China

^b National Supercomputer Center in Tianjin, Tianjin, 300451, China

[‡] Shaobing Zhang and Shuning Li contributed equally to this work.

* Email: lingliu@bit.edu.cn, zhangxiuhui@bit.edu.cn.

Section S1. Computational methods

S1.1 Quantum chemical calculation methods

S1.2 Universal force field (UFF)

S1.3. Introduction of thermodynamic functions calculation

Section S2. Cluster formation pathways

Section S3. Some information about Atmospheric Cluster Dynamics

Code (ACDC) simulation

Section S4. Figures and Tables

Fig. S1 The electrostatic potential (ESP)-mapped molecular van der Waals (vdW) surfaces of HIO₃ molecule at the ω B97X-D/6-311++G(3df,3pd) (for O, H) + aug-cc-pVTZ-PP with ECP28MDF (for I) level of theory. The unit is kcal mol⁻¹. The blue and yellow dots represent the minimum and maximum points of the ESP, respectively. The white, red and purple spheres represent the H, O and I atoms, respectively.

Fig. S2 The most stable configurations of (HIO₃)₁₋₆ clusters identified at the ω B97X-D/6-311++G(3df,3pd) (for O, H) + aug-cc-pVTZ-PP with ECP28MDF (for I) level of theory. The white, red and purple spheres represent the H, O and I atoms, respectively. The black dashed lines represent the hydrogen bonds (HBs) or halogen bonds (XBs) formed between HIO₃ molecules, and the bond lengths of HBs are indicated by black numbers, the bond lengths of XBs are indicated by blue numbers. The bond lengths are given in Å.

Fig. S3 The cluster formation pathway of the self-nucleation of HIO₃ at 268.15, 278.15, 288.15 and 298.15 K and different [HIO₃] (10⁷, 10⁸ and 10⁹ molecules cm⁻³).

Fig. S4 Actual Gibbs free energies of formation (ΔG_{actual}) of clusters at different [HIO₂] (2×10^5 , 2×10^6 and 2×10^7 molecules cm⁻³) and (a) 268.15 K, (b) 288.15 K and (c) 298.15 K. The solid, dashed and dotted lines correspond to the paths growing through collision with HIO₂, (HIO₂)₂ and (HIO₂)₃, respectively.

Fig. S5 Actual Gibbs free energies of formation (ΔG_{actual}) of clusters at different $[\text{HIO}_3]$ (10^7 , 10^8 and 10^9 molecules cm^{-3}) and (a) 268.15 K, (b) 278.15 K, (c) 288.15 K and (d) 298.15 K.

Fig. S6 The time-dependent concentration (cm^{-3}) of clusters and the time-dependent formation rate ($\text{cm}^{-3} \text{s}^{-1}$) of clusters growing out of the simulation system at 268.15, 278.15, 288.15 and 298.15 K. The I and IA are the abbreviations of HIO_2 and HIO_3 , respectively.

Table S1 The values of thermodynamic functions of each molecule/cluster involved in this study at the RI-CC2/aug-cc-pVTZ (for O, H) + aug-cc-pVTZ-PP with ECP28MDF (for I) // $\omega\text{B97X-D/6-311++G(3df,3pd)}$ (for O, H) + aug-cc-pVTZ-PP with ECP28MDF (for I) level of theory at 268.15, 278.15, 288.15 and 298.15 K.

Table S2 Cartesian coordinates of clusters involved in this study optimized at the $\omega\text{B97XD/6-311++G(3df,3pd)}$ (for O, H) + aug-cc-pVTZ-PP with ECP28MDF (for I) level of theory. All coordinates are given in Å.

Table S3 The ratio of the collision frequencies between the clusters and monomer molecule at the concentration C to the total evaporation frequencies of clusters ($\beta \cdot C / \Sigma \gamma$) of $(\text{HIO}_2)_{2-6}$ clusters and $(\text{HIO}_3)_{2-6}$ clusters at the RI-CC2/aug-cc-pVTZ (for O, H) + aug-cc-pVTZ-PP with ECP28MDF (for I) // $\omega\text{B97X-D/6-311++G(3df,3pd)}$ (for O, H) + aug-cc-pVTZ-PP with ECP28MDF (for I) level of theory at 268.15, 288.15 and 298.15 K and $P = 1$ atm. $C_1 = 2 \times 10^6$ molecules cm^{-3} for $(\text{HIO}_2)_{2-6}$ clusters, $C_2 = 1 \times 10^8$ molecules cm^{-3} for $(\text{HIO}_3)_{2-6}$ clusters.

Table S4 The bond lengths of HIO_3 molecule in this study and three different polymorphs ($\alpha\text{-HIO}_3$, $\beta\text{-HIO}_3$, $\gamma\text{-HIO}_3$). The values are shown in Å.

Table S5 The thermal contribution to Gibbs free energy of formation ($\Delta G_{\text{thermal}}$) for $(\text{HIO}_2)_2$ and $(\text{HIO}_2)_3$ clusters by harmonic approximation calculations ($\Delta G_{\text{t-harm}}$) and anharmonic calculations ($\Delta G_{\text{t-anharm}}$) at the $\omega\text{B97X-D/6-311++G(3df,3pd)}$ (for O, H) + aug-cc-pVTZ-PP with ECP28MDF (for I) level of theory.

Section S5. References

Section S1. Computational methods

S1.1 Quantum chemical calculation methods

We have carried out some tests to prove the reliability of the quantum chemical methods used in our study. Firstly, in our previous work about the nucleation mechanisms of HIO₃ in clean and polluted coastal regions,¹ the performance of ω B97X-D and several other methods including M06-2X, B3LYP-D3, PBE-D3, PW91, and MP2 were compared. The results showed that the average absolute difference and the maximum difference between the Gibbs free energy of formation (ΔG) by ω B97X-D method and those by CCSD(T) single-point correction were the smallest. Thus, ω B97X-D method is excellent in calculating the ΔG of clusters. Besides, we have compared the bond lengths of HIO₃ molecule in this study with the experimentally measured bond lengths of HIO₃ in three different polymorphs (α -HIO₃, β -HIO₃, γ -HIO₃).²⁻⁴ As shown in Table S4, the bond lengths of HIO₃ molecule in this study are close to those measured experimentally. Therefore, the structures optimized at the ω B97X-D/6-311++G(3df,3pd) (for O, H) + aug-cc-pVTZ-PP with ECP28MDF (for I) level of theory are reliable. In summary, the methods used in our study are reliable.

Besides, in the calculation of the thermal contribution to ΔG , we used the harmonic approximation, in which only the second order derivative of the energy was included and higher terms in the Taylor expansion of the potential energy were neglected. Although considering anharmonicity is more accurate than harmonic approximation, it is more computationally consuming due to the consideration of higher-order terms in the Taylor expansion. To evaluate the rationality of harmonic approximation used in this study, we have compared the thermal contribution to Gibbs free energy of formation ($\Delta G_{\text{thermal}}$) for (HIO₂)₂ and (HIO₂)₃ clusters by harmonic approximation calculations and anharmonic calculations. As can be seen from Table S5, the $\Delta G_{\text{thermal}}$ by harmonic approximation calculations are very close to those by anharmonic calculations and the absolute differences between them are lower than 0.01 kcal mol⁻¹ (0.0094 and 0.0075 kcal mol⁻¹). Such small variation of $\Delta G_{\text{thermal}}$ would almost have no effect on the simulation results, such as the cluster formation rates, the steady-state concentrations of clusters and the cluster formation pathways. Therefore, considering the minor difference between the results and the more computationally demanding of anharmonic calculations, we use the harmonic approximation in the present study.

S1.2 Universal force field (UFF)

In the selection of the initial clusters, the Universal force field (UFF)⁵ was used to obtain the energies of all initial guessed structures generated by ABCluster program,^{6,7} and then the up to 1000 structures with relatively low energies were selected from the initial guessed structures for further optimization. In UFF, the potential energy⁵ of a molecule is expressed as:

$$E = E_R + E_\theta + E_\phi + E_\omega + E_{\text{vdw}} + E_{\text{el}} \quad (\text{S1})$$

where E_R is the bond stretching interaction, E_θ is the bond angle bending interaction, E_ϕ is the dihedral angle torsion interaction, E_ω is the inversion interaction, E_{vdw} is the van der Waals interaction and E_{el} is the electrostatic interaction.

S1.3. Introduction of thermodynamic functions calculation

The thermal contribution to Gibbs free energy can be approximated as sum of several terms involving translational (trans), rotational (rot), vibrational (vib) and electronic (ele) contributions by ignoring their coupling. The detailed explanations are shown below and the values of the corresponding thermodynamic functions for each molecule/cluster are shown in Table S1.

The common thermodynamic functions include internal energy (U), enthalpy (H), entropy (S) and Gibbs free energy (G). The following two equations are well known.

$$H = U + PV \quad (\text{S2})$$

$$G = H - TS \quad (\text{S3})$$

where T is temperature, P is pressure and V is volume.

In Gaussian, systems are treated as the ideal gas and the thermodynamic functions are given per mole when the molecular vibration analysis are performed. In this case,

$$PV = RT \quad (\text{S4})$$

$$H = U + RT \quad (\text{S5})$$

where $R = 8.314 \text{ J}\cdot(\text{mol}\cdot\text{K})^{-1}$ is the ideal gas constant.

Besides, the most critical quantity in statistical thermodynamics is the molecular partition function (q), which is dimensionless. The expression of q is:

$$q = \sum_i^\infty g_i e^{(-\epsilon_i/k_B T)} \quad (\text{S6})$$

where ϵ_i is the energy of the molecular energy level i , g_i is the degeneracy of energy level i , and k_B is the Boltzmann constant.

Various thermodynamic functions can be calculated from the q , such as the U and S :

$$U = k_B T^2 \left(\frac{\partial \ln q}{\partial T} \right)_{N,V} \quad (\text{S7})$$

$$S = k_B T \left(\frac{\partial \ln q}{\partial T} \right)_{N,V} + k_B \ln q \quad (\text{S8})$$

As shown in equation (1) in the manuscript, the Gibbs free energy of formation of clusters is calculated as:

$$\Delta G = \Delta E_{\text{RI-CC2}} + \Delta G_{\text{thermal}}^{\omega\text{B97X-D}}$$

where $\Delta E_{\text{RI-CC2}}$ is the electronic contribution calculated at the RI-CC2/aug-cc-pVTZ (for O, H) + aug-cc-pVTZ-PP with ECP28MDF (for I) level of theory, and $\Delta G_{\text{thermal}}^{\omega\text{B97X-D}}$ is the thermal contribution obtained at the $\omega\text{B97X-D}/6\text{-}311\text{++G}(3\text{df},3\text{pd})$ (for O, H) + aug-cc-pVTZ-PP with ECP28MDF (for I) level of theory. Similarly, the Gibbs free energy of each molecule/cluster can be written as:

$$G = E_{\text{RI-CC2}} + G_{\text{thermal}}^{\omega\text{B97X-D}} \quad (\text{S9})$$

The thermodynamic functions can be approximated as sum of several terms involving translational (trans), rotational (rot), vibrational (vib) and electronic (ele) contributions by ignoring their coupling.

$$G_{\text{thermal}} = G_{\text{trans}} + G_{\text{rot}} + G_{\text{vib}} + G_{\text{ele}} \quad (\text{S10})$$

$$U_{\text{thermal}} = U_{\text{trans}} + U_{\text{rot}} + U_{\text{vib}} + U_{\text{ele}} \quad (\text{S11})$$

$$H_{\text{thermal}} = H_{\text{trans}} + H_{\text{rot}} + H_{\text{vib}} + H_{\text{ele}} \quad (\text{S12})$$

$$S = S_{\text{trans}} + S_{\text{rot}} + S_{\text{vib}} + S_{\text{ele}} \quad (\text{S13})$$

The H_{thermal} and U_{thermal} only differ by their translation parts:

$$H_{\text{trans}} = U_{\text{trans}} + RT \quad (\text{S14})$$

And the q can be written as the product of several terms:

$$q = q_{\text{trans}} q_{\text{rot}} q_{\text{vib}} q_{\text{ele}} \quad (\text{S15})$$

The translational partition function (q_{trans}) of a molecule/cluster is calculated as:

$$q_{\text{trans}} = \left(\frac{2\pi m k_B T}{h^2} \right)^{3/2} V = \left(\frac{2\pi m k_B T}{h^2} \right)^{3/2} \frac{k_B T}{P} \quad (\text{S16})$$

where m is the mass of the molecule/cluster and h is the Plank constant.

The rotational partition function (q_{rot}) is calculated as:

$$q_{\text{rot}} = \frac{8\pi^2 I k_B T}{\sigma h^2} \quad (\text{linear molecule}) \quad (\text{S17})$$

$$q_{\text{rot}} = \frac{8\pi^2}{\sigma h^3} (2\pi k_B T)^{3/2} \sqrt{I_1 I_2 I_3} \quad (\text{nonlinear molecule}) \quad (\text{S18})$$

where σ is the rotational symmetry factor and I_i are the principal moments of inertia.

In harmonic approximation, the vibrational partition function (q_{vib}) can be written as:

$$q_{\text{vib}} = \prod_i^{3N-6} \frac{e^{-hv_i/(2k_B T)}}{1 - e^{-hv_i/(k_B T)}} \quad (\text{S19})$$

where v_i is the vibrational frequency of vibration mode i , and there are $3N-5$ vibrational modes for linear molecules.

The electronic partition function (q_{ele}) is calculated as:

$$q_{\text{ele}} = \sum_i^{\infty} g_i e^{(-\epsilon_i/k_B T)} \quad (\text{S20})$$

where ϵ_i is the electronic energy level i with respect to ground state.

In Gaussian, it is assumed that the first electronic excitation energy is much greater than $k_B T$, the first and higher excited states are inaccessible at any temperature. Further, the energy of the ground state is set to zero. Hence, these assumptions simplify the q_{ele} to $q_{\text{ele}} = g_0$.

Based on equations (S7), (S8) and (S16) - (S20), we can obtain the U_{trans} , U_{rot} , U_{vib} , U_{ele} , S_{trans} , S_{rot} , S_{vib} , and S_{ele} . Then we can obtain G_{trans} , G_{rot} , G_{vib} , and G_{ele} for a molecule/cluster based on equation (S3), equation (S5) and equation (S14):

$$G_{\text{trans}} = -RT \ln \left[\left(\frac{2\pi m k_B T}{h^2} \right)^{3/2} \frac{k_B T}{P} \right] \quad (\text{S21})$$

$$G_{\text{rot}} = -RT \ln \left[\frac{8\pi^2}{\sigma h^3} (2\pi k_B T)^{3/2} \sqrt{I_1 I_2 I_3} \right] \quad (\text{S22})$$

$$G_{\text{vib}} = R \sum_i^{3N-6} \left(\frac{hv_i}{2k_B} + T \ln [1 - e^{-hv_i/k_B T}] \right) \quad (\text{S23})$$

$$G_{\text{ele}} = -RT \ln g_0 \quad (\text{S24})$$

Section S2. Cluster formation pathways

As shown in Fig. 7, as for the cluster formation pathways of the self-nucleation of HIO_2 , the contribution for growing out of the simulated system of each path is slightly different under different T (268.15, 278.15, 288.15 and 298.15 K) and different $[\text{HIO}_2]$ (2×10^5 , 2×10^6 and 2×10^7 molecules cm^{-3}).

Firstly, at a moderate HIO_2 concentration ($[\text{HIO}_2] = 2 \times 10^6$ molecules cm^{-3}), the contribution of each path would be different at different T . At a low temperature of 268.15 K, the contributions of these three paths are the same as those at 278.15 K. When the temperature increases from 278.15 K to 298.15 K, the contribution of the $(\text{HIO}_2)_6$ -driven path (path 1) is almost the same, the contribution of the $(\text{HIO}_2)_5$ -driven path (path 2) decreases from 18% to 8% and the contribution of the $(\text{HIO}_2)_4$ -driven path (path 3) increases from 11% to 22%.

Furthermore, in order to explore the influence of the concentration of nucleation precursors, the main formation paths at 278.15 K under different $[\text{HIO}_2]$ are investigated in Fig. 7. As the $[\text{HIO}_2]$ increases from 2×10^5 to 2×10^7 molecules cm^{-3} , the contribution of the $(\text{HIO}_2)_4$ -driven path (path 3) does not change, the contribution of the $(\text{HIO}_2)_5$ -driven path (path 2) increases from 16% to 23% and the contribution of the $(\text{HIO}_2)_6$ -driven path (path 1) decreases from 72% to 66%.

Section S3. Some information about Atmospheric Cluster Dynamics

Code (ACDC) simulation

The ACDC used in this study is version 2016-03-19. In ACDC, the birth-death equations are solved with the ode15s routine in MATLAB program.⁸ The total propagation time of each ACDC simulation performed in this study was 20000 seconds, during which all simulations had reached the steady state. The MATLAB solver uses an adaptive step size, so the interval of the time points is not uniform, that is, the time step is not a definite value. During the total simulation time of 20000 s, a total of 30018 time points were outputted. In the initial simulation time of 0.1 s, the interval of the output time points is 1×10^{-5} s. In the simulation time ranging from 0.1 s to 2 s, the interval of the output time points is 0.1 s, and in the simulation time ranging from 2 s to 20000 s, the interval of the output time points is 1 s. Besides, the time-dependent concentration (cm^{-3}) of clusters and the time-dependent formation rate ($\text{cm}^{-3} \text{ s}^{-1}$) of clusters growing out of the simulation system at different temperatures and different precursor concentrations are shown in Fig. S6.

Section S4. Figures and Tables

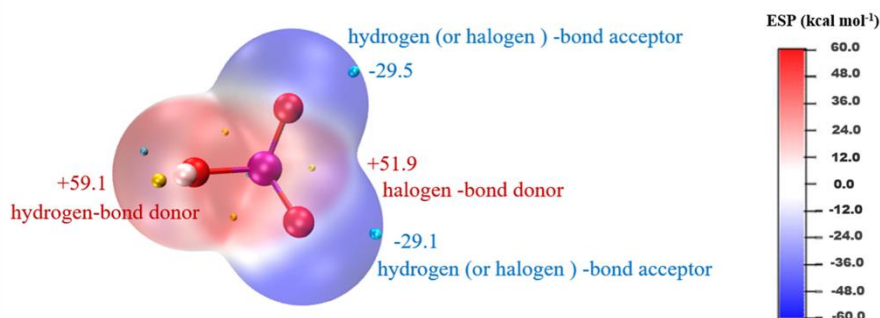


Fig. S1 The electrostatic potential (ESP)-mapped molecular van der Waals (vdW) surfaces of HIO_3 molecule at the $\omega\text{B97X-D/6-311++G(3df,3pd)}$ (for O, H) + aug-cc-pVTZ-PP with ECP28MDF (for I) level of theory. The unit is kcal mol^{-1} . The blue and yellow dots represent the minimum and maximum points of the ESP, respectively. The white, red and purple spheres represent the H, O and I atoms, respectively.

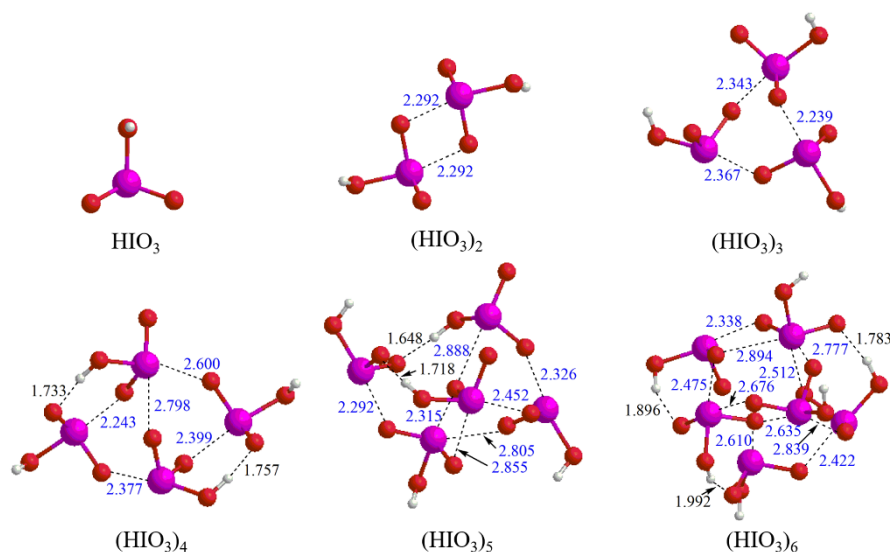


Fig. S2 The most stable configurations of $(\text{HIO}_3)_{1-6}$ clusters identified at the $\omega\text{B97X-D/6-311++G(3df,3pd)}$ (for O, H) + aug-cc-pVTZ-PP with ECP28MDF (for I) level of theory. The white, red and purple spheres represent the H, O and I atoms, respectively. The black dashed lines represent the hydrogen bonds (HBs) or halogen bonds (XBs) formed between HIO_3 molecules, and the bond lengths of HBs are indicated by black numbers, the bond lengths of XBs are indicated by blue numbers. The bond lengths are given in Å.

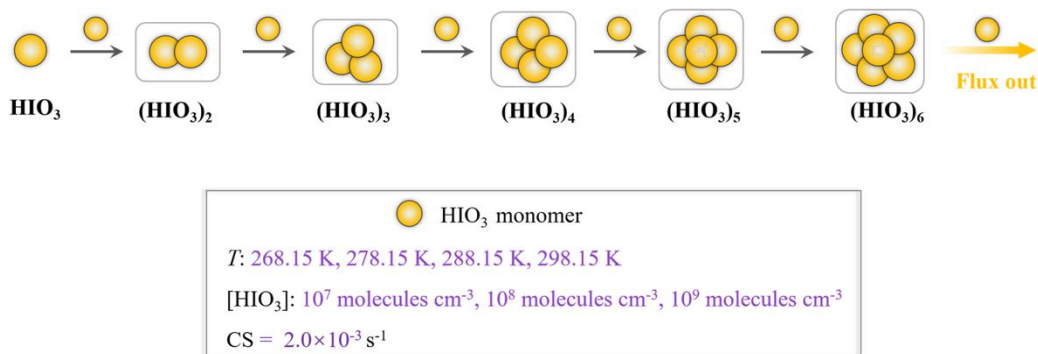
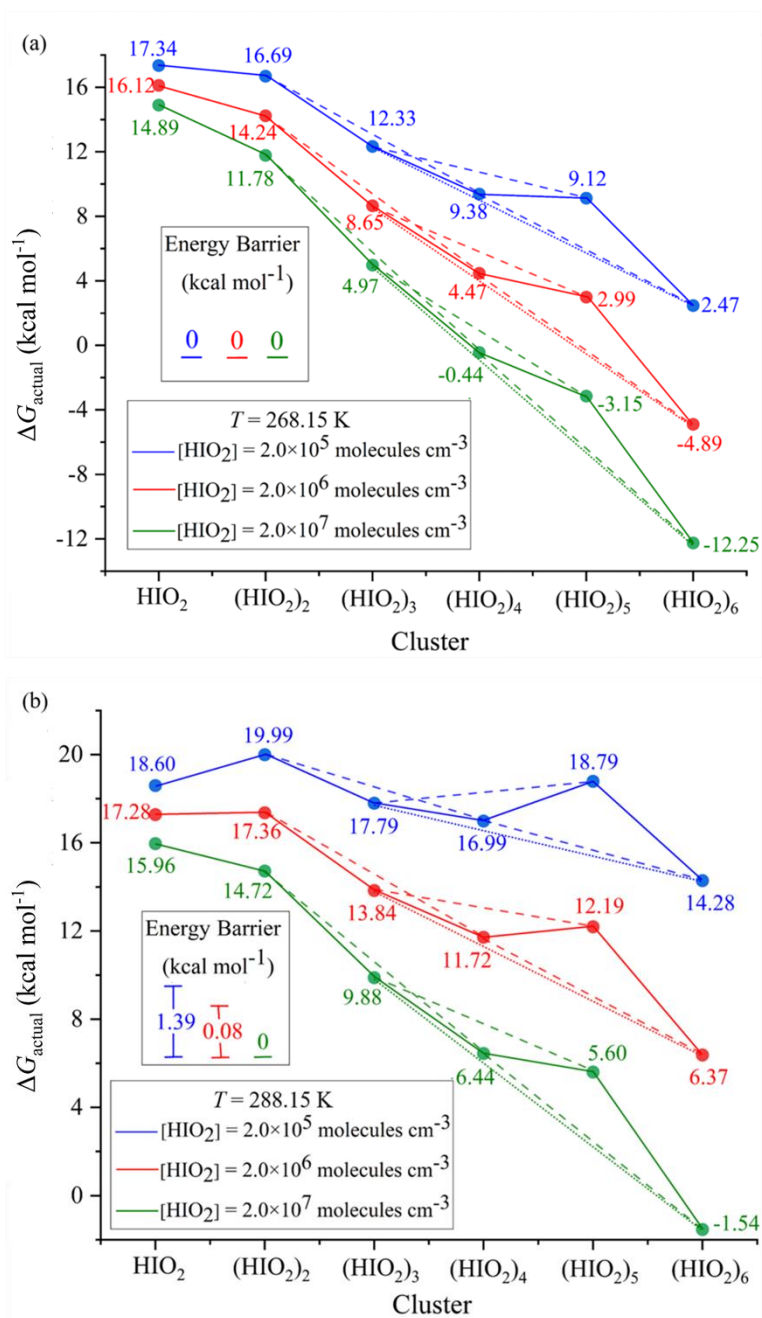


Fig. S3 The cluster formation pathway of the self-nucleation of HIO_3 at 268.15, 278.15, 288.15 and 298.15 K and different $[\text{HIO}_3]$ (10^7 , 10^8 and 10^9 molecules cm^{-3}).



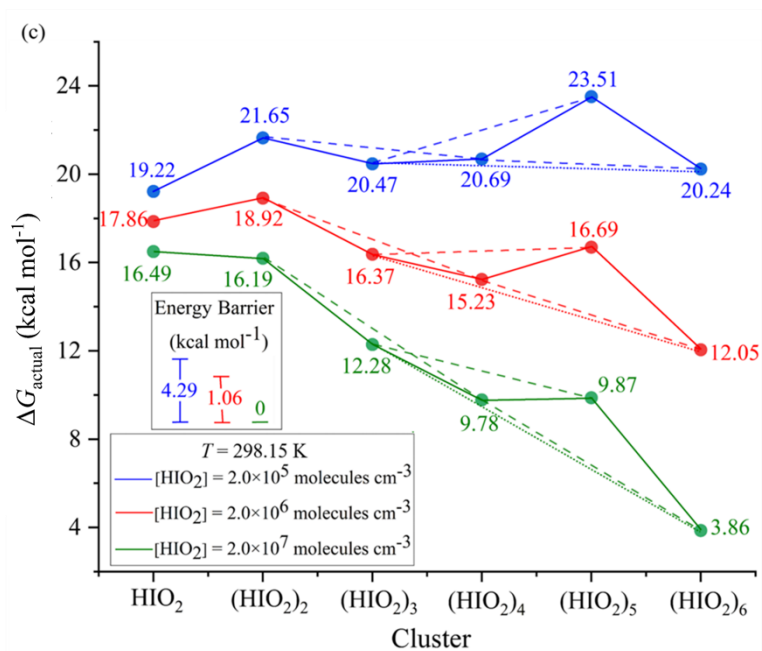
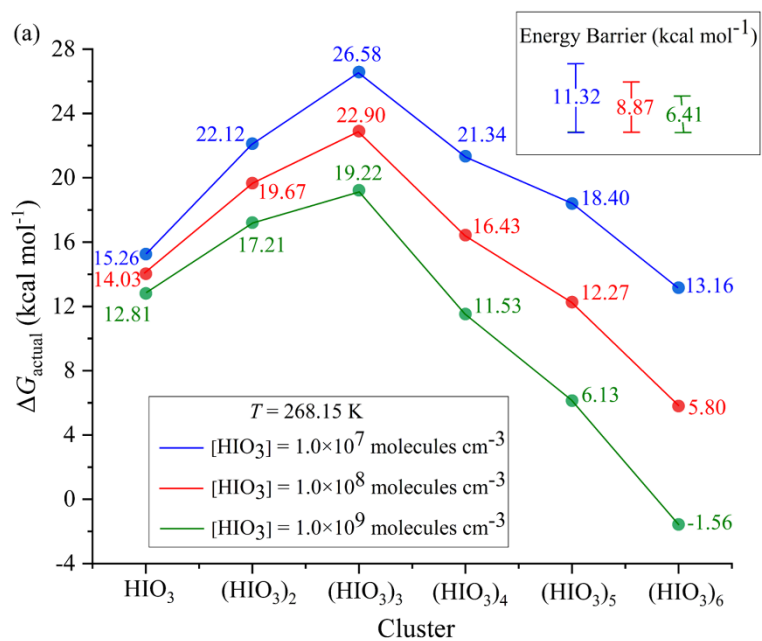
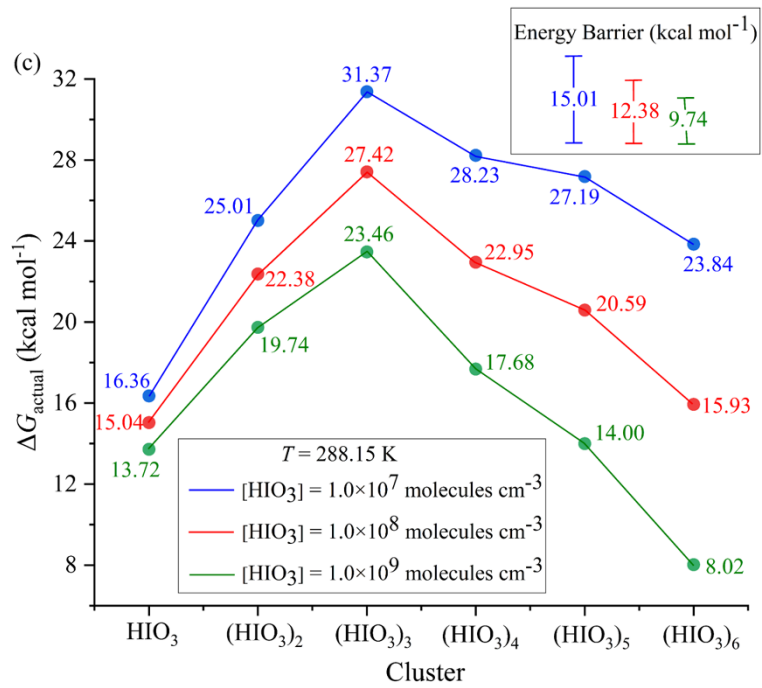
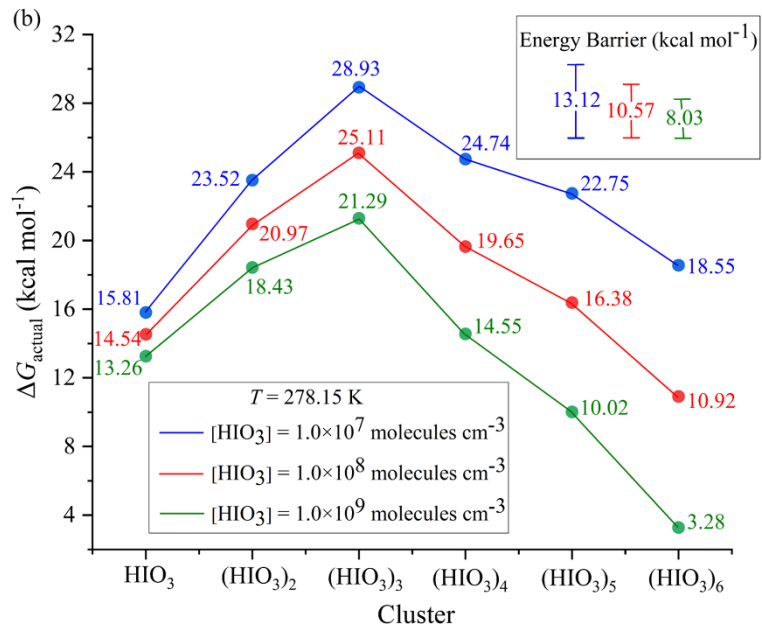


Fig. S4 Actual Gibbs free energies of formation (ΔG_{actual}) of clusters at different $[\text{HIO}_2]$ (2×10^5 , 2×10^6 and 2×10^7 molecules cm^{-3}) and (a) 268.15 K, (b) 288.15 K and (c) 298.15 K. The solid, dashed and dotted lines correspond to the paths growing through collision with HIO_2 , $(\text{HIO}_2)_2$ and $(\text{HIO}_2)_3$, respectively.





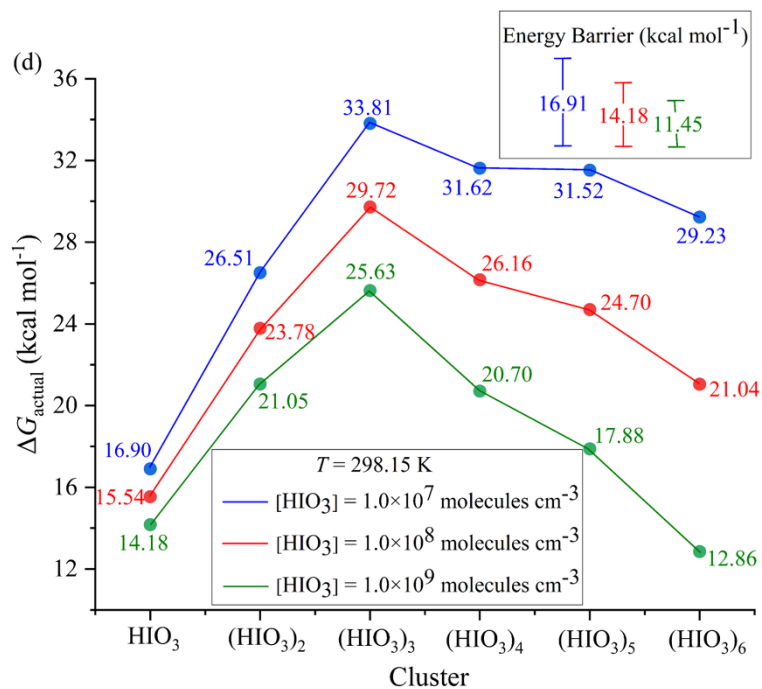
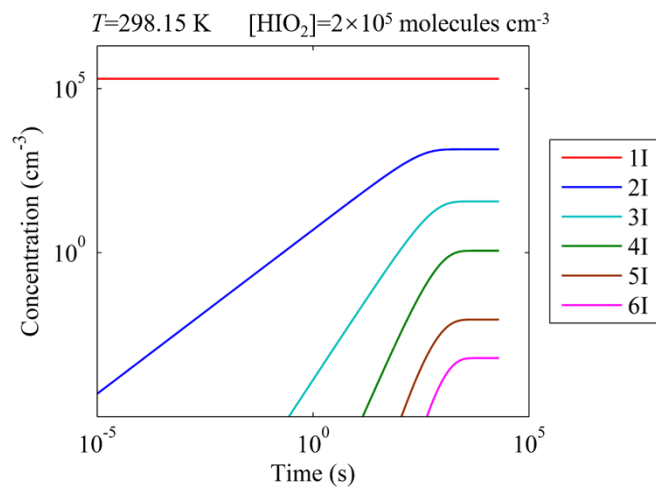
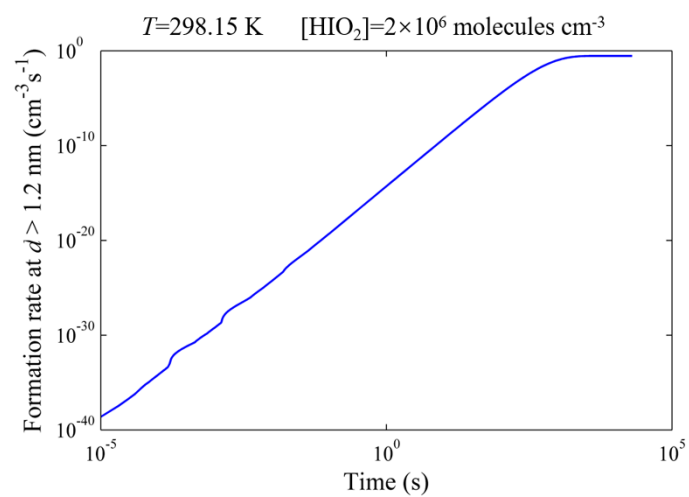
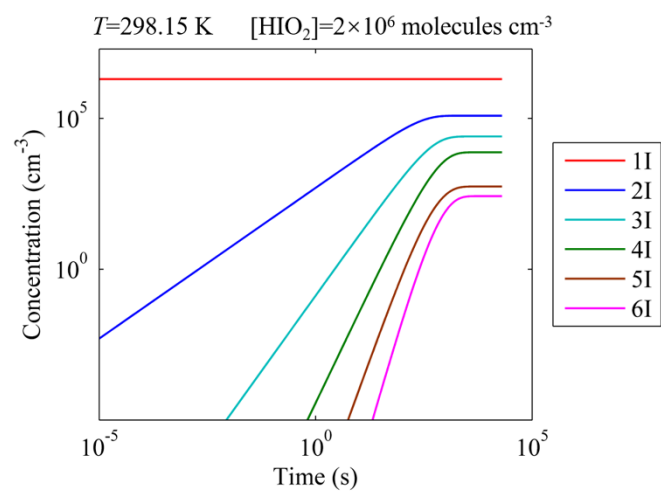
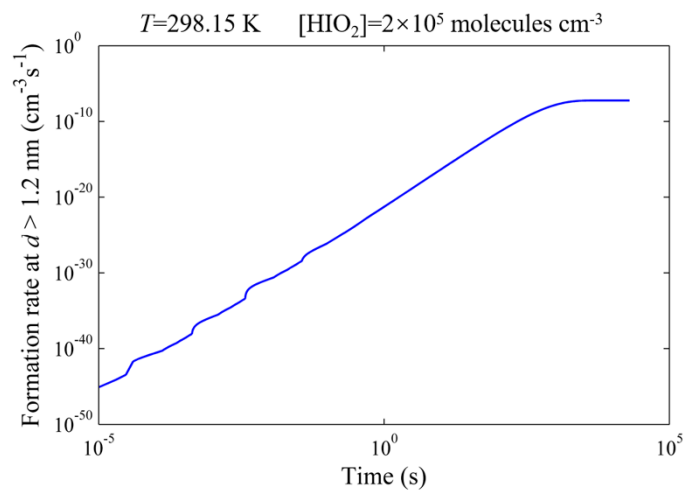
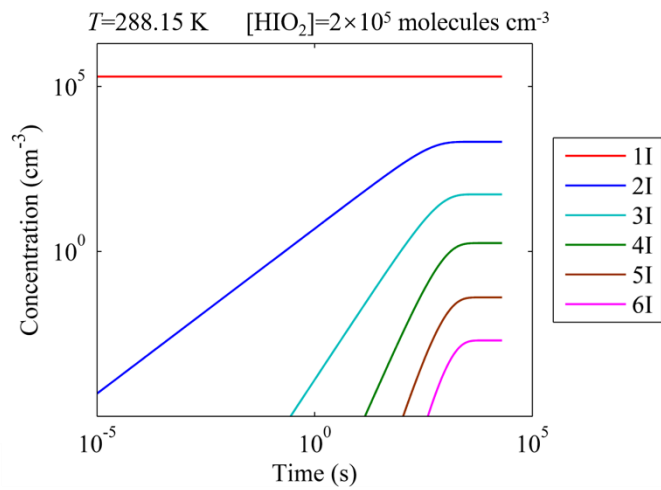
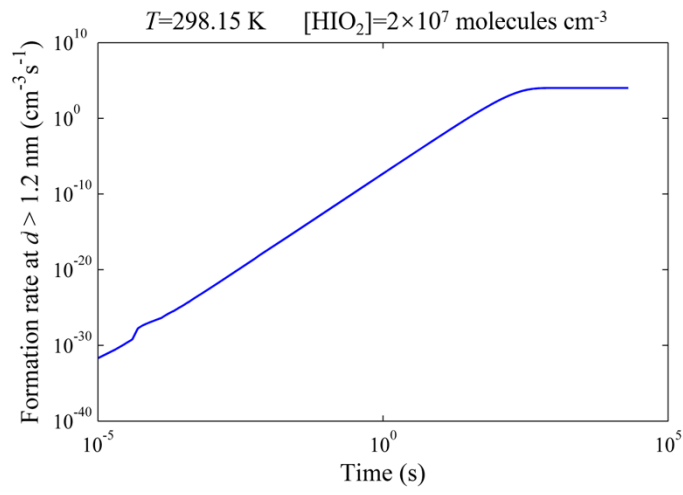
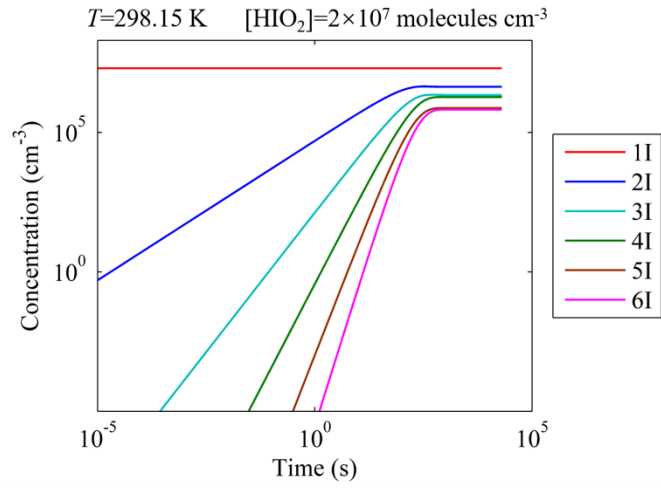
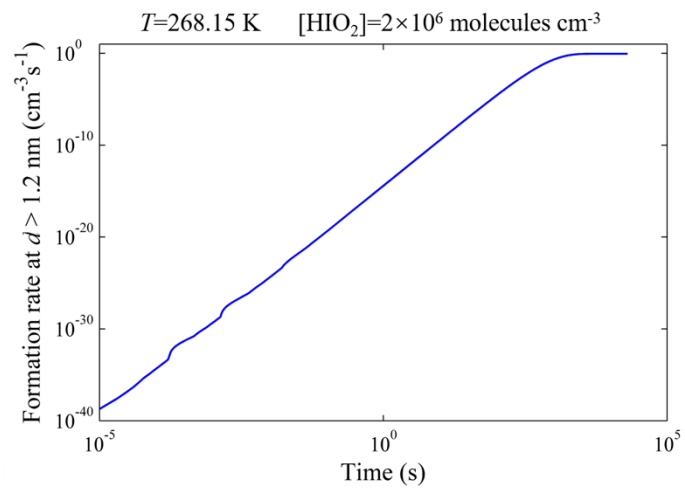
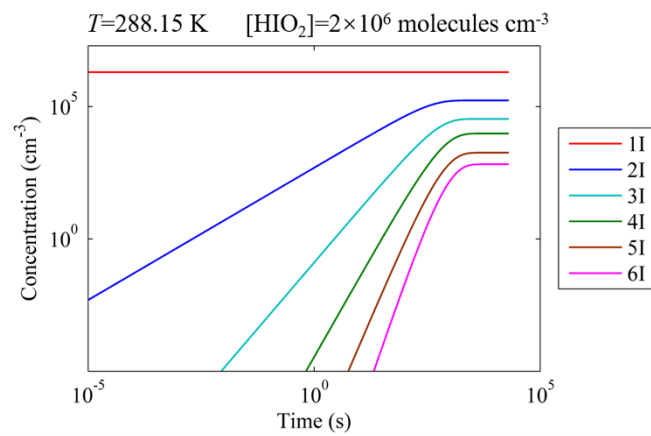
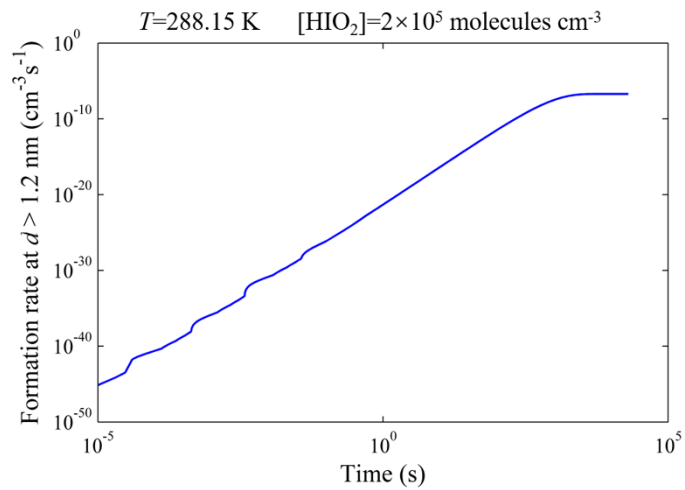


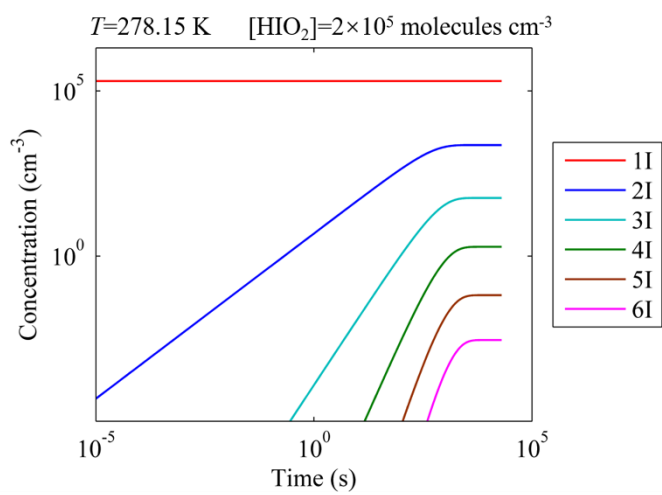
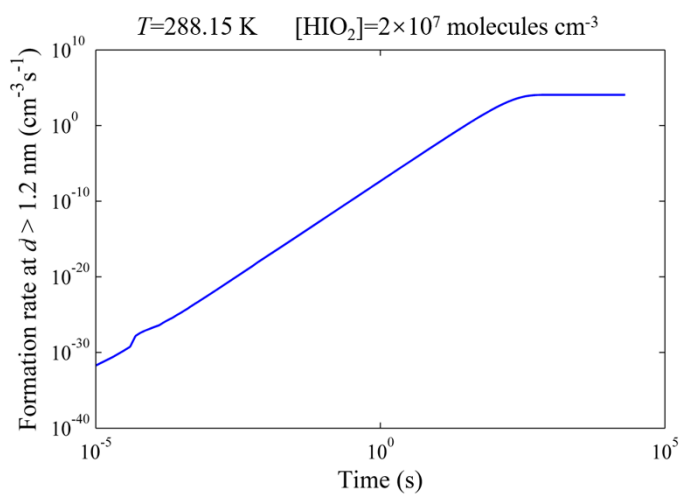
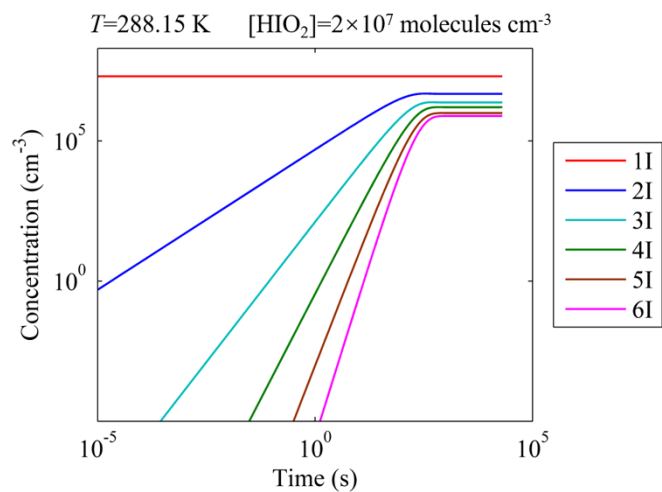
Fig. S5 Actual Gibbs free energies of formation (ΔG_{actual}) of clusters at different [HIO₃] (10^7 , 10^8 and 10^9 molecules cm⁻³) and (a) 268.15 K, (b) 278.15 K, (c) 288.15 K and (d) 298.15 K.

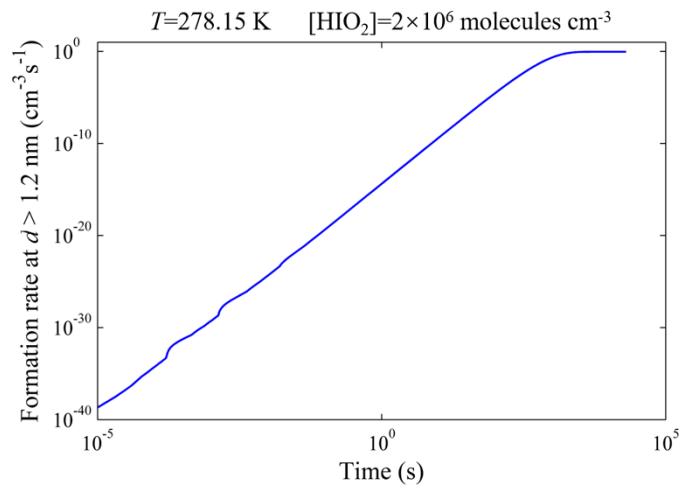
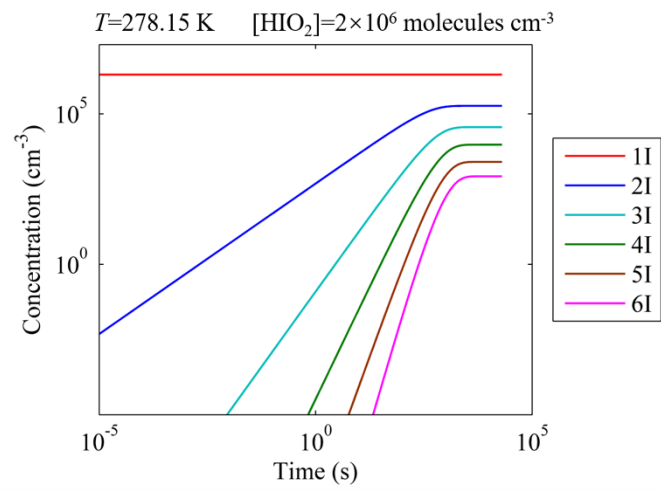
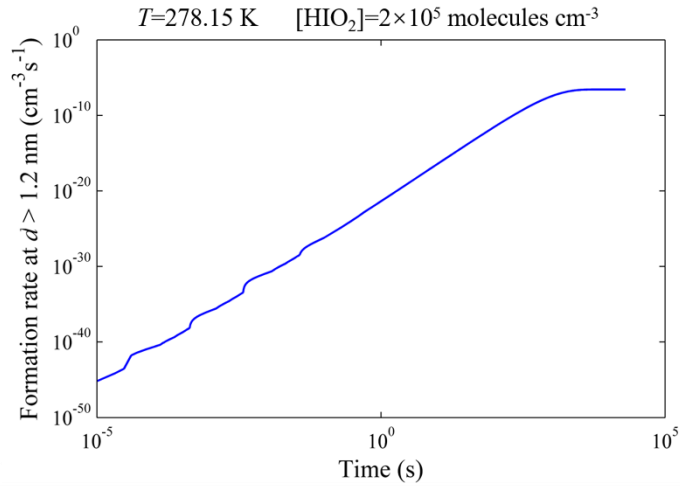


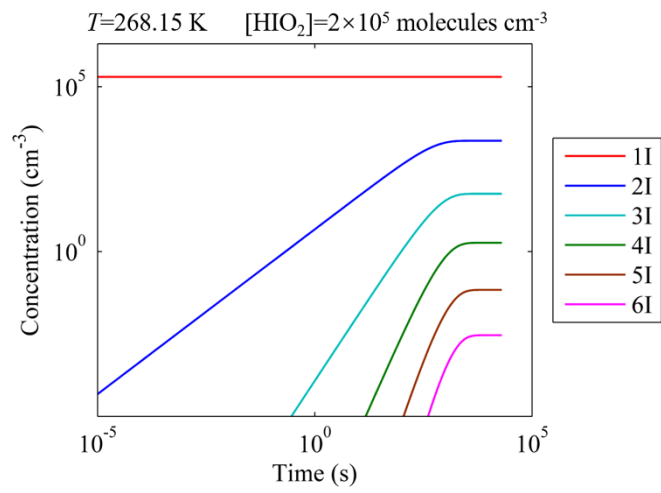
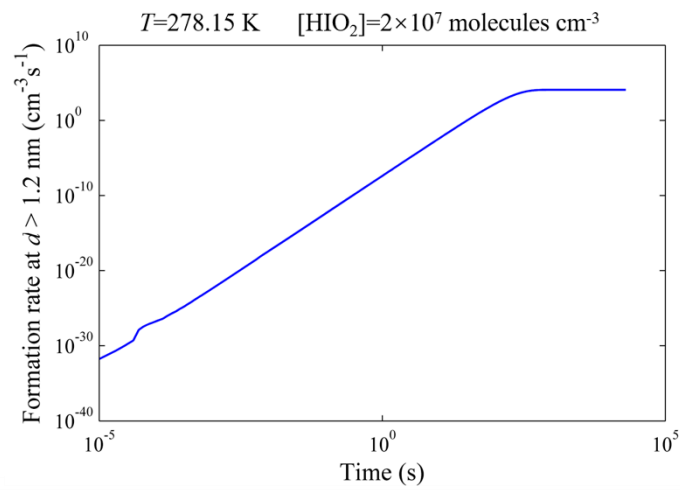
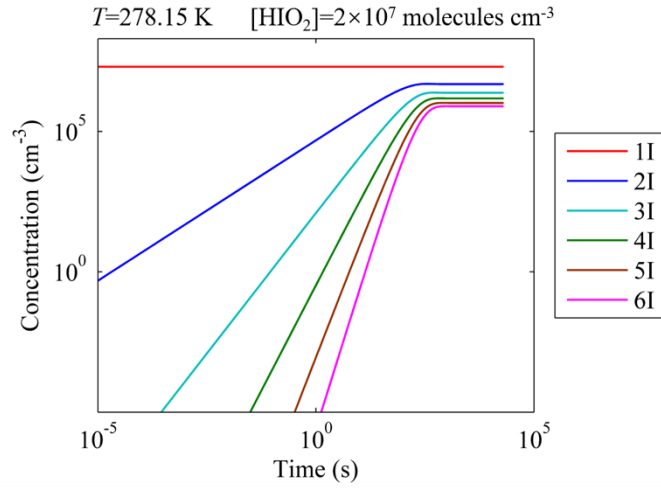


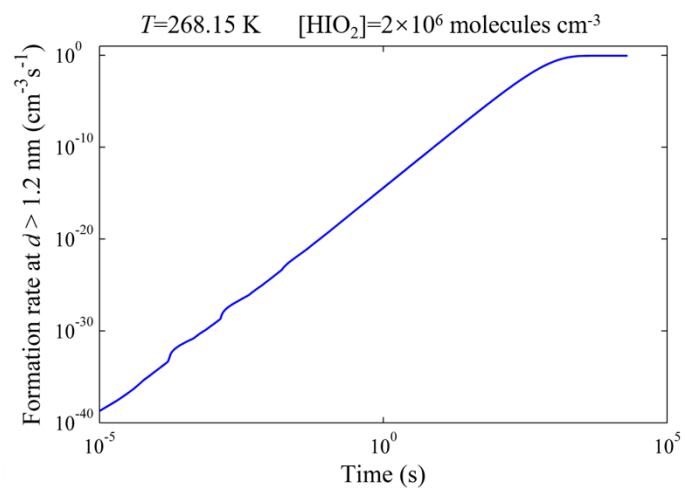
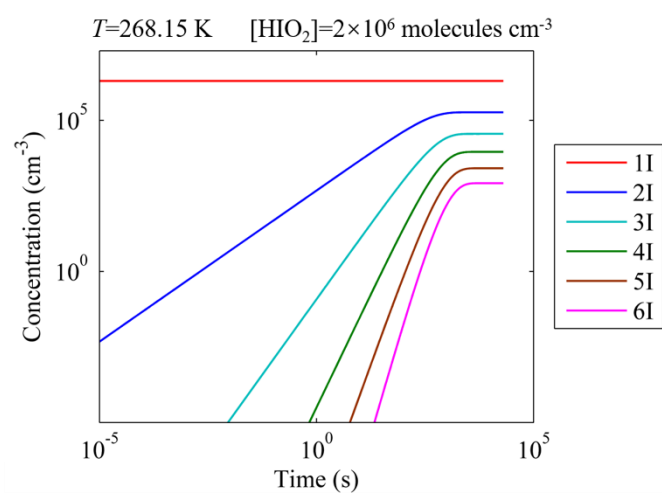
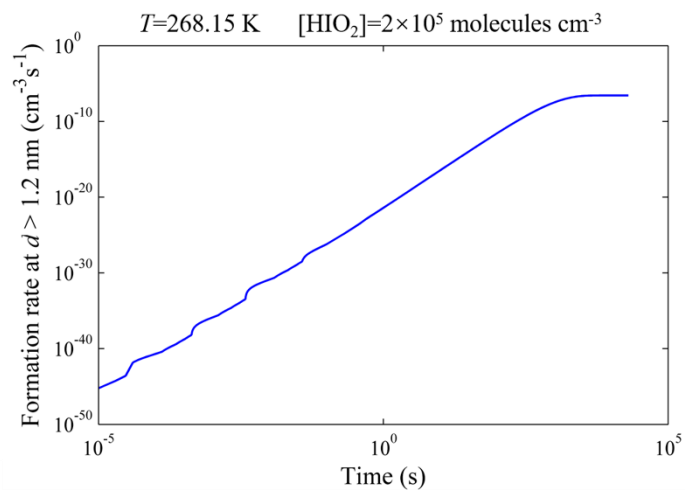


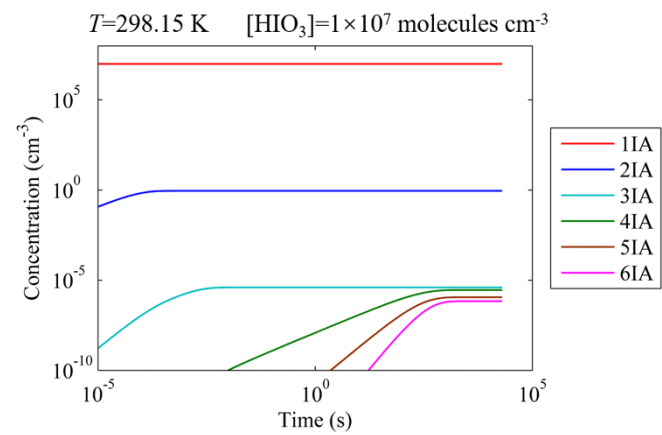
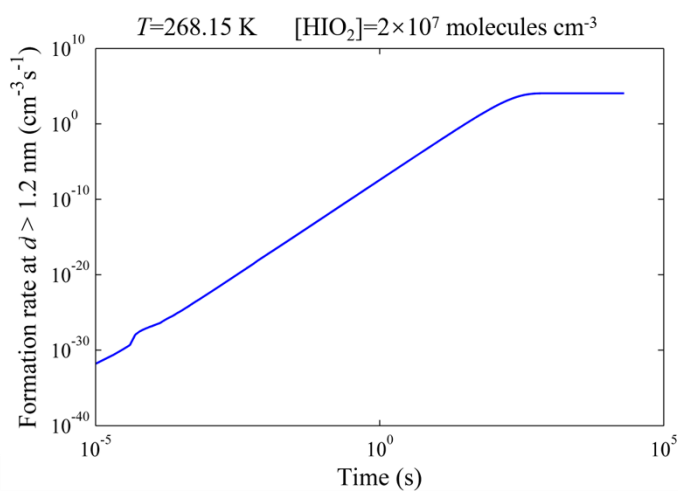
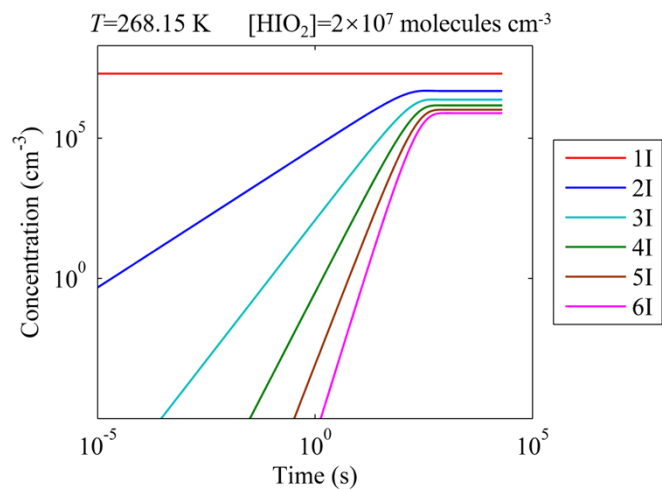


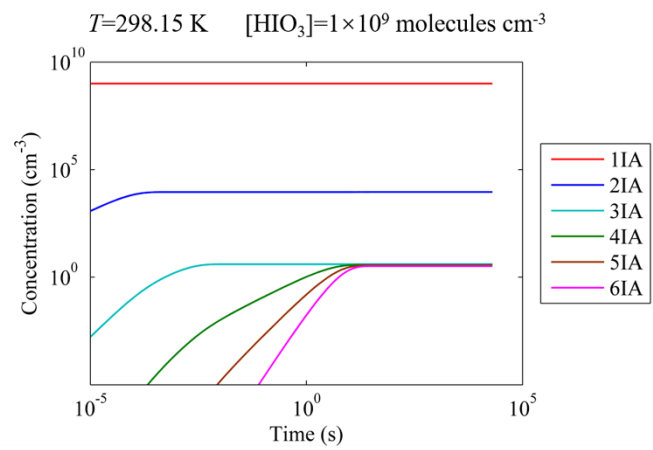
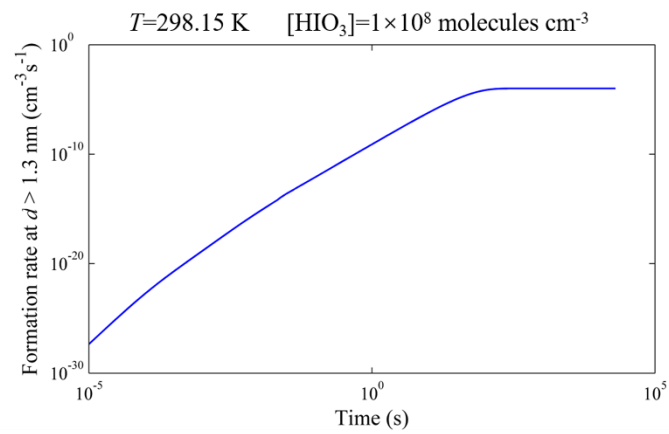
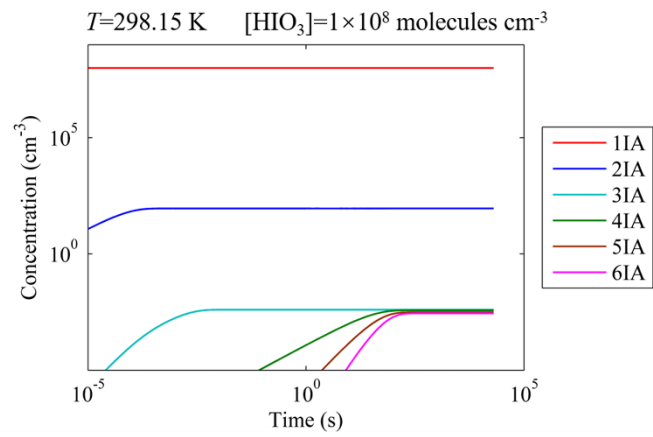
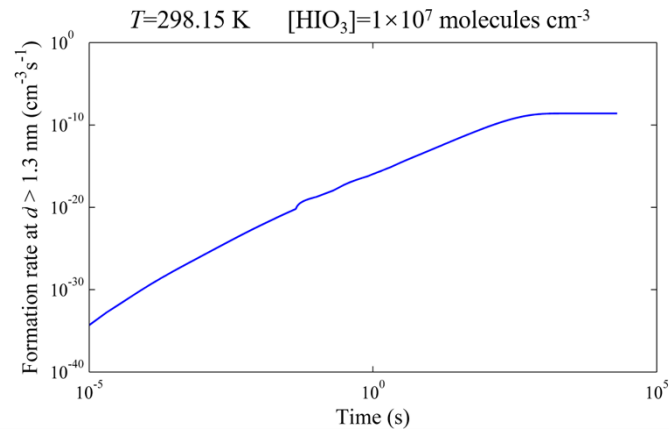


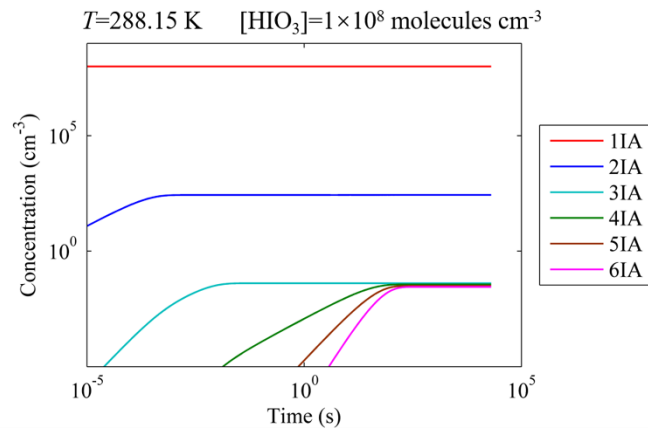
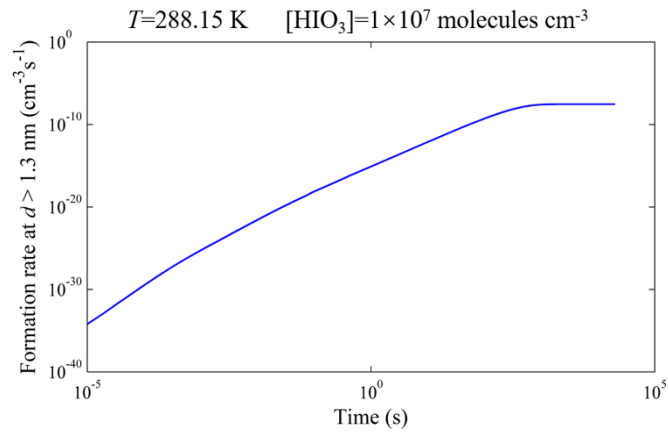
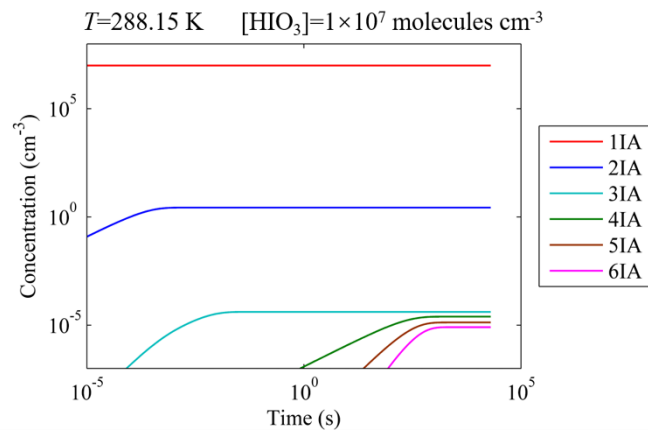
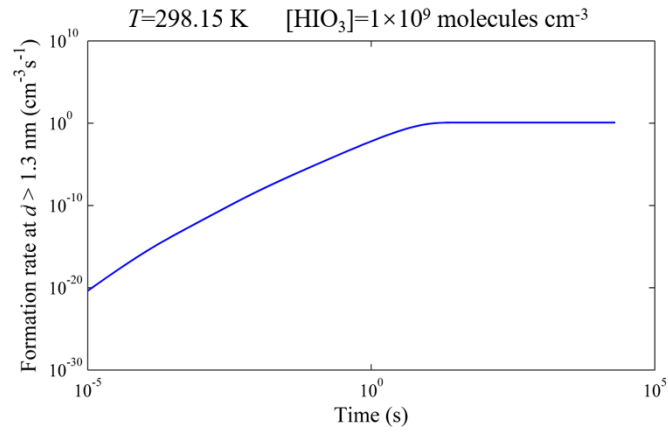


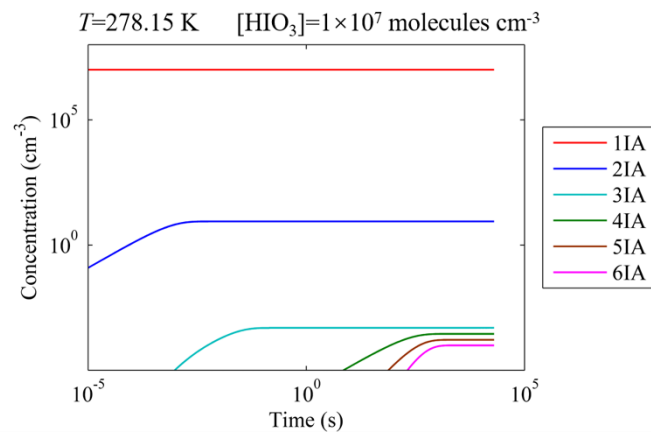
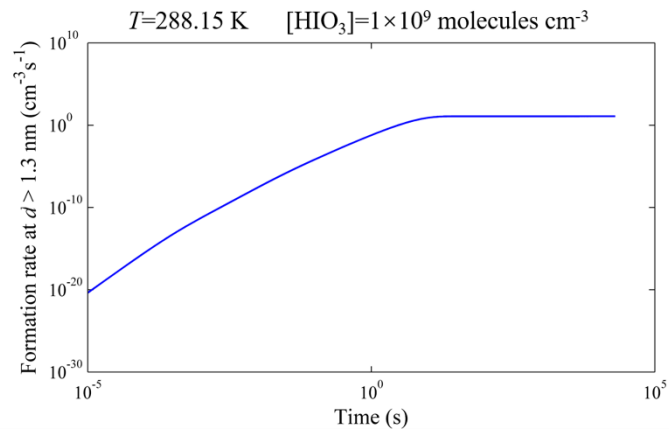
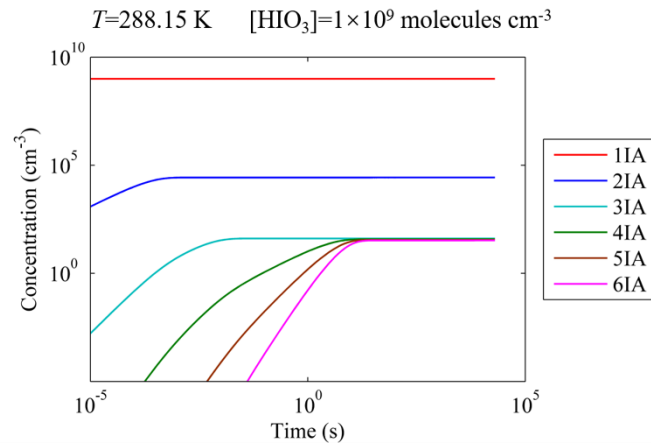
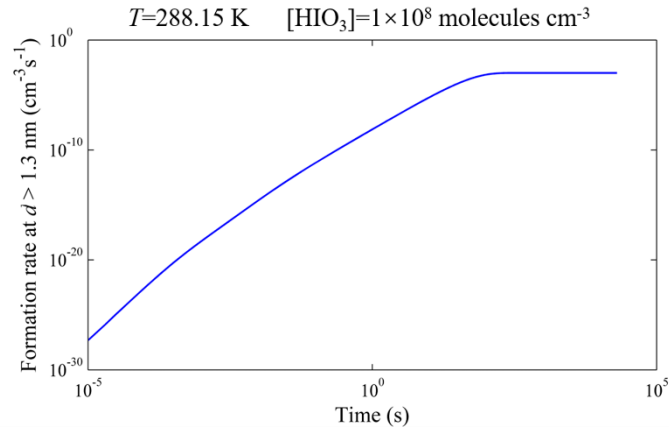


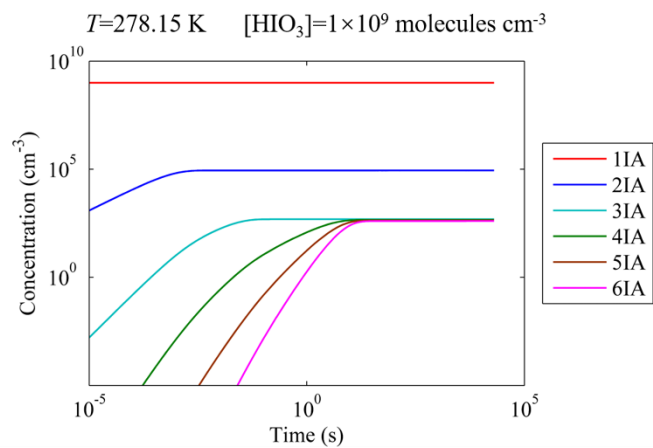
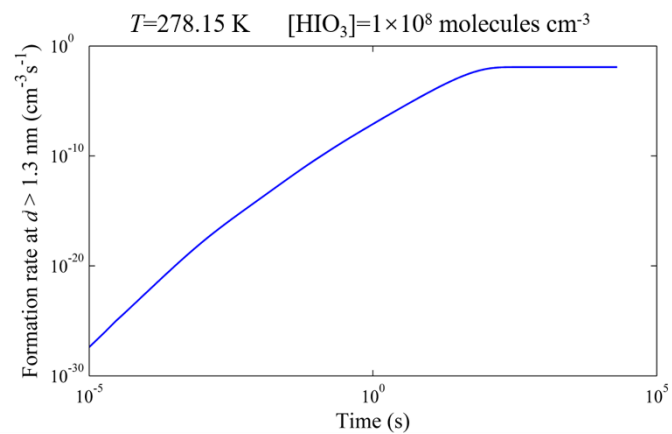
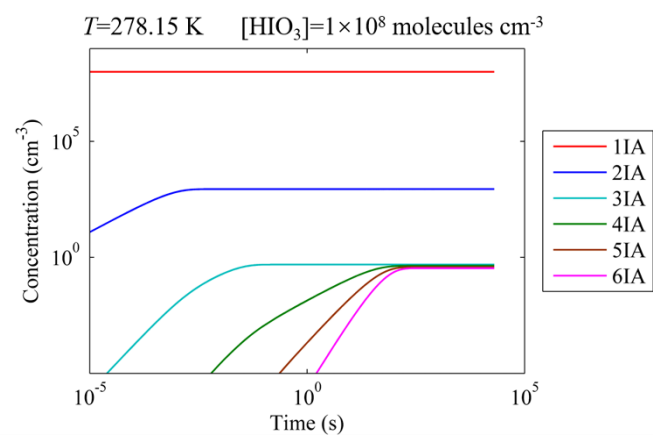
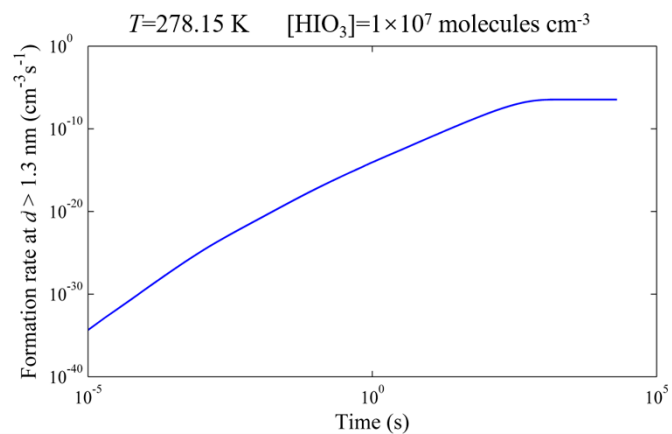


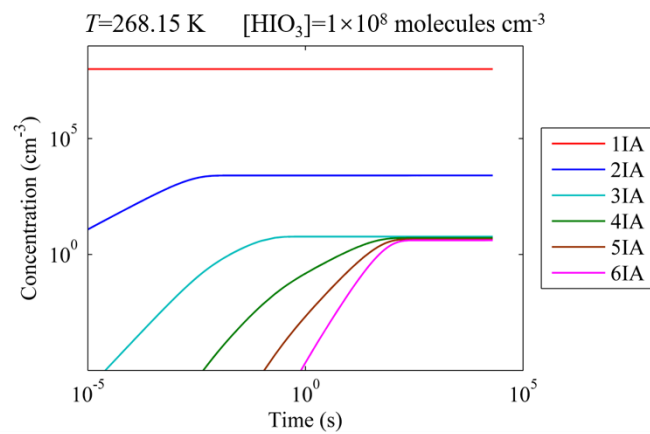
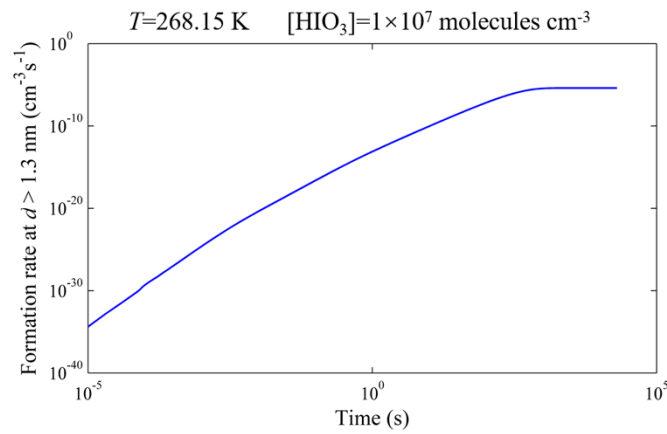
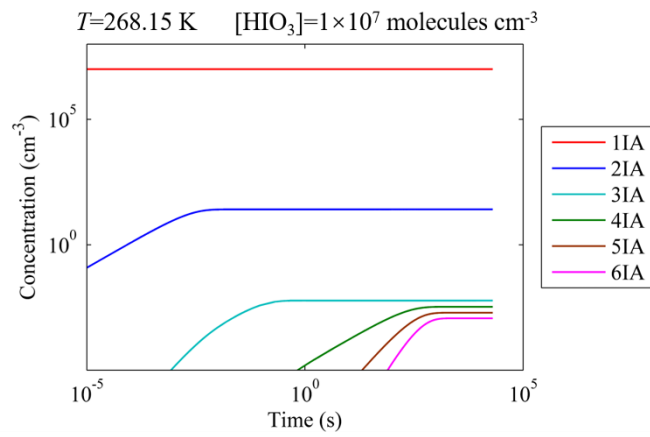
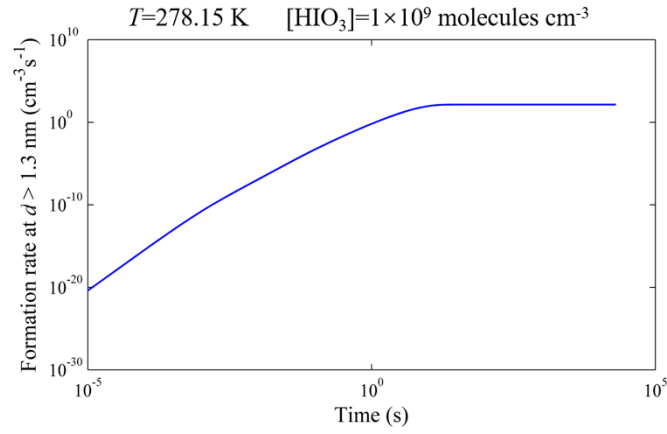












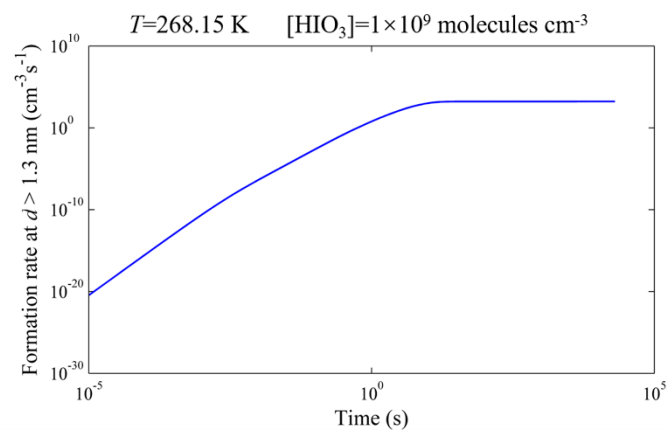
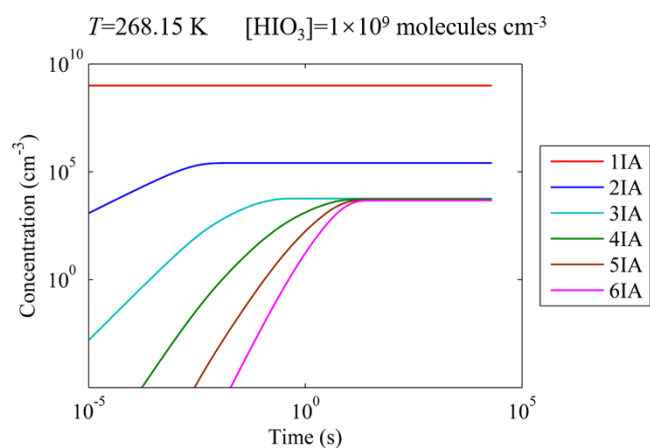
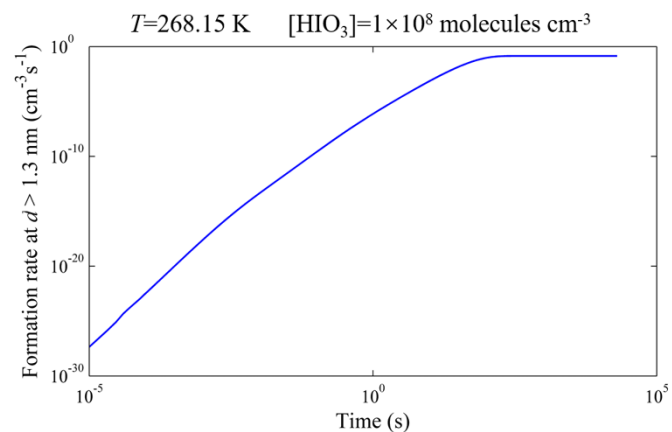


Fig. S6 The time-dependent concentration (cm^{-3}) of clusters and the time-dependent formation rate ($\text{cm}^{-3} \text{s}^{-1}$) of clusters growing out of the simulation system at 268.15, 278.15, 288.15 and 298.15 K. The I and IA are the abbreviations of HIO_2 and HIO_3 , respectively.

Table S1 The values of thermodynamic functions of each molecule/cluster involved in this study at the RI-CC2/aug-cc-pVTZ (for O, H) + aug-cc-pVTZ-PP with ECP28MDF (for I) // ω B97X-D/6-311++G(3df,3pd) (for O, H) + aug-cc-pVTZ-PP with ECP28MDF (for I) level of theory at 268.15, 278.15, 288.15 and 298.15 K.

$T = 298.15$ K							
Cluster	G_{trans}	G_{rot}	G_{vib}	G_{ele}	G_{thermal}	E	ΔG
	(kcal mol ⁻¹)	(hartree)	(hartree)	(kcal mol ⁻¹)			
HIO ₂	-10.8	-6.3	9.5	0.0	-0.012043	-447.608021	
(HIO ₂) ₂	-11.4	-8.0	17.8	0.0	-0.002693	-895.264212	-16.8
(HIO ₂) ₃	-11.8	-9.1	25.7	0.0	0.007686	-1342.927094	-37.2
(HIO ₂) ₄	-12.0	-9.2	32.0	0.0	0.017147	-1790.586909	-56.2
(HIO ₂) ₅	-12.2	-10.0	39.3	0.0	0.027227	-2238.243188	-72.6
(HIO ₂) ₆	-12.4	-10.3	48.0	0.0	0.040271	-2685.912229	-95.1
HIO ₃	-10.9	-6.7	11.1	0.0	-0.010357	-522.731543	
(HIO ₃) ₂	-11.5	-8.3	20.2	0.0	0.000629	-1045.496116	-7.3
(HIO ₃) ₃	-11.8	-9.3	29.2	0.0	0.012844	-1568.265465	-16.9
(HIO ₃) ₄	-12.1	-9.8	38.3	0.0	0.026013	-2091.051036	-36.0
(HIO ₃) ₅	-12.3	-10.2	46.5	0.0	0.038283	-2613.832234	-53.0
(HIO ₃) ₆	-12.5	-10.4	55.7	0.0	0.052345	-3136.618794	-72.2

$T = 288.15$ K							
Cluster	G_{trans}	G_{rot}	G_{vib}	G_{ele}	G_{thermal}	E	ΔG
	(kcal mol ⁻¹)	(hartree)	(hartree)	(kcal mol ⁻¹)			
HIO ₂	-10.4	-6.1	9.6	0.0	-0.010947	-447.608021	
(HIO ₂) ₂	-11.0	-7.7	18.0	0.0	-0.001159	-895.264212	-17.2
(HIO ₂) ₃	-11.3	-8.8	26.1	0.0	0.009626	-1342.927094	-38.0

(HIO ₂) ₄	-11.6	-8.9	32.7	0.0	0.019519	-1790.586909	-57.4
(HIO ₂) ₅	-11.8	-9.6	40.2	0.0	0.030038	-2238.243188	-74.2
(HIO ₂) ₆	-11.9	-10.0	49.1	0.0	0.043412	-2685.912229	-97.3
HIO ₃	-10.5	-6.4	11.1	0.0	-0.009212	-522.731543	
(HIO ₃) ₂	-11.0	-8.0	20.5	0.0	0.002336	-1045.496116	-7.7
(HIO ₃) ₃	-11.4	-8.9	29.8	0.0	0.015038	-1568.265465	-17.7
(HIO ₃) ₄	-11.6	-9.5	39.1	0.0	0.028667	-2091.051036	-37.2
(HIO ₃) ₅	-11.8	-9.8	47.6	0.0	0.041412	-2613.832234	-54.6
(HIO ₃) ₆	-12.0	-10.0	57.1	0.0	0.055926	-3136.618794	-74.3

$T = 278.15$ K

Cluster	G_{trans}	G_{rot}	G_{vib}	G_{ele}	G_{thermal}	E	ΔG
	(kcal mol ⁻¹)	(hartree)	(hartree)	(kcal mol ⁻¹)			
HIO ₂	-10.0	-5.8	9.6	0.0	-0.009858	-447.608021	
(HIO ₂) ₂	-10.5	-7.4	18.2	0.0	0.000359	-895.264212	-17.6
(HIO ₂) ₃	-10.9	-8.4	26.6	0.0	0.01154	-1342.927094	-38.9
(HIO ₂) ₄	-11.1	-8.5	33.4	0.0	0.021857	-1790.586909	-58.7
(HIO ₂) ₅	-11.3	-9.3	41.1	0.0	0.032806	-2238.243188	-75.9
(HIO ₂) ₆	-11.4	-9.6	50.2	0.0	0.046504	-2685.912229	-99.4
HIO ₃	-10.0	-6.2	11.2	0.0	-0.008075	-522.731543	
(HIO ₃) ₂	-10.6	-7.7	20.9	0.0	0.004023	-1045.496116	-8.1
(HIO ₃) ₃	-10.9	-8.6	30.4	0.0	0.0172	-1568.265465	-18.5
(HIO ₃) ₄	-11.2	-9.1	39.9	0.0	0.031279	-2091.051036	-38.5
(HIO ₃) ₅	-11.4	-9.4	48.7	0.0	0.044488	-2613.832234	-56.3
(HIO ₃) ₆	-11.5	-9.7	58.5	0.0	0.059444	-3136.618794	-76.3

$T = 268.15 \text{ K}$							
Cluster	G_{trans}	G_{rot}	G_{vib}	G_{ele}	G_{thermal}	E	ΔG
	(kcal mol ⁻¹)	(hartree)	(hartree)	(kcal mol ⁻¹)			
HIO ₂	-9.6	-5.6	9.6	0.0	-0.008776	-447.608021	
(HIO ₂) ₂	-10.1	-7.2	18.4	0.0	0.001859	-895.264212	-18.0
(HIO ₂) ₃	-10.4	-8.1	27.0	0.0	0.013428	-1342.927094	-39.7
(HIO ₂) ₄	-10.7	-8.2	34.0	0.0	0.02416	-1790.586909	-60.0
(HIO ₂) ₅	-10.8	-8.9	42.0	0.0	0.035529	-2238.243188	-77.6
(HIO ₂) ₆	-11.0	-9.2	51.3	0.0	0.049543	-2685.912229	-101.6
HIO ₃	-9.6	-5.9	11.2	0.0	-0.006946	-522.731543	
(HIO ₃) ₂	-10.2	-7.4	21.2	0.0	0.005688	-1045.496116	-8.4
(HIO ₃) ₃	-10.5	-8.3	30.9	0.0	0.019329	-1568.265465	-19.2
(HIO ₃) ₄	-10.7	-8.8	40.7	0.0	0.033849	-2091.051036	-39.7
(HIO ₃) ₅	-10.9	-9.1	49.8	0.0	0.04751	-2613.832234	-57.9
(HIO ₃) ₆	-11.1	-9.3	59.8	0.0	0.062896	-3136.618794	-78.4

Table S2 Cartesian coordinates of clusters involved in this study optimized at the ω B97XD/6-311++G(3df,3pd) (for O, H) + aug-cc-pVTZ-PP with ECP28MDF (for I) level of theory. All coordinates are given in Å.

HIO ₂	X	Y	Z
I	-0.091005	-0.272143	0.004432
O	-1.303898	1.076515	-0.009899
O	1.668980	0.610105	-0.114677
H	1.902634	0.930647	0.761721

$(\text{HIO}_2)_2$	X	Y	Z
I	-1.578005	-0.342023	0.004952
O	-0.465797	1.204395	-0.014294
O	-3.215025	0.775918	-0.107780
H	-3.344733	1.243767	0.720830
I	1.578004	0.342023	-0.004952
O	0.465797	-1.204395	0.014313
O	3.215027	-0.775916	0.107762
H	3.344725	-1.243765	-0.720849

$(\text{HIO}_2)_3$	X	Y	Z
I	1.034301	1.812493	-0.138034
O	1.038215	0.325454	1.024048
O	3.009617	2.045907	-0.008725
H	3.240087	2.410997	0.848773
I	-2.075886	-0.082773	-0.065971
O	-1.161073	1.541124	-0.337339
O	-3.622700	0.841067	0.776172
H	-4.111208	1.334343	0.112943
I	1.062650	-1.733667	0.198919
O	-0.295445	-1.115784	-0.961111
O	0.853078	-3.616641	-0.415373
H	1.181128	-3.705127	-1.313536

$(\text{HIO}_2)_4$	X	Y	Z
I	1.589996	1.644184	0.814407
O	0.580663	1.589996	-0.769866
O	1.442150	3.629986	0.981002

H	1.997986	4.052519	0.322198
I	-1.589996	-1.644184	0.814407
O	-0.580663	-1.589996	-0.769866
O	-1.442150	-3.629986	0.981002
H	-1.997986	-4.052519	0.322198
I	-1.644184	1.589996	-0.814407
O	-1.589996	0.580663	0.769866
O	-3.629986	1.442150	-0.981002
H	-4.052519	1.997986	-0.322198
I	1.644184	-1.589996	-0.814407
O	1.589996	-0.580663	0.769866
O	3.629986	-1.442150	-0.981002
H	4.052519	-1.997986	-0.322198

(HIO ₂) ₅	X	Y	Z
I	-0.111615	2.398712	-0.027476
O	-1.078372	1.459715	-1.326890
O	-1.697617	3.338899	0.705027
H	-2.162026	2.704737	1.262596
I	-2.926866	0.279349	-0.862435
O	-2.346470	0.261545	0.924542
O	-4.496938	-0.893062	-0.505086
H	-5.169127	-0.397958	-0.031104
I	0.964444	-1.984298	-1.246409
O	1.915197	-1.385113	0.272205
O	2.590700	-1.946141	-2.401321
H	3.129794	-2.720004	-2.221689
I	-0.903909	-1.288176	1.787171
O	-0.841892	-2.024534	0.062582

O	0.369558	-2.605250	2.527360
H	1.222284	-2.402475	2.122169
I	2.965722	0.618272	0.333527
O	1.689787	1.252599	-0.876709
O	3.810041	2.404342	0.602481
H	4.315039	2.647152	-0.177531

(HIO ₂) ₆	X	Y	Z
I	-3.208496	1.502906	-0.035878
O	-1.425045	1.745869	-0.537229
O	-3.812593	3.296943	-0.628687
H	-3.527627	3.963731	0.001160
I	-2.384141	-2.181280	-0.280063
O	-2.647883	-0.599447	0.742416
O	-2.906842	-3.304514	1.266000
H	-2.186330	-3.311969	1.905447
I	2.212011	1.988497	0.170900
O	2.262877	0.724899	1.574993
O	0.684344	2.981479	0.945101
H	-0.121480	2.638421	0.512528
I	-0.319914	0.149146	-2.003959
O	-1.929021	-0.827701	-1.994568
O	0.768481	-1.133372	-2.980438
H	1.350036	-1.526445	-2.291206
I	0.359971	-0.185050	2.352900
O	0.936181	-1.826959	1.539399
O	-1.250163	-1.072924	3.030313
H	-1.932376	-0.922649	2.344661
I	3.935483	-1.113942	-0.481934

O	3.833014	0.745273	-0.768808
O	2.177278	-1.686903	-0.735264
H	1.362340	-1.676886	0.637386

HIO ₃	X	Y	Z
I	-0.097221	0.004930	-0.243095
O	-0.843163	-1.345650	0.628433
O	-0.527112	1.503114	0.602173
O	1.779550	-0.182280	0.231752
H	1.878526	-0.062776	1.185167

(HIO ₃) ₂	X	Y	Z
I	1.605051	0.108932	0.259818
O	1.996597	1.471483	-0.792799
O	0.473803	-0.943145	-0.745717
O	3.140569	-1.017258	-0.123688
H	3.259854	-1.115740	-1.075118
I	-1.605050	-0.108931	-0.259817
O	-0.473803	0.943139	0.745725
O	-1.996605	-1.471483	0.792796
O	-3.140566	1.017263	0.123683
H	-3.259856	1.115744	1.075113

(HIO ₃) ₃	X	Y	Z
I	1.551191	-1.444560	0.241428
O	2.027934	-0.540904	-1.220886
O	-0.184068	-1.901175	-0.058596
O	2.255350	-3.153174	-0.362216

H	2.182802	-3.219929	-1.320845
I	0.661501	1.889676	-0.207204
O	0.911557	0.550911	1.031477
O	-0.293274	3.072479	0.689289
O	2.394831	2.710999	0.099161
H	2.353969	3.213962	0.921573
I	-2.190212	-0.646210	-0.103985
O	-1.258387	0.719624	-0.867328
O	-2.135654	-0.385353	1.640565
O	-3.930295	0.140912	-0.447962
H	-4.032198	0.949384	0.068569

(HIO ₃) ₄	X	Y	Z
I	2.924189	0.043511	-0.863546
O	3.495044	-0.674501	0.671117
O	1.971392	1.475080	-0.368773
O	4.569386	0.974814	-1.276430
H	4.924013	1.390013	-0.481182
I	0.231749	-2.007131	0.795648
O	-0.071305	-0.531514	1.744680
O	1.025820	-1.417148	-0.729522
O	1.839477	-2.593365	1.645114
H	2.553603	-1.945466	1.436317
I	-0.325952	2.052848	0.703478
O	-1.064348	1.090490	-0.685768
O	-0.242071	3.680434	0.040526
O	-1.932455	2.214762	1.723876
H	-2.600100	1.568527	1.392064
I	-2.804464	-0.305610	-0.914476

O	-3.546657	0.382929	0.555057
O	-1.855288	-1.727989	-0.307803
O	-4.363628	-1.363303	-1.384538
H	-4.833129	-1.630395	-0.585993

(HIO ₃) ₅	X	Y	Z
I	-3.534410	0.130841	-0.286420
O	-2.310683	0.486044	-1.557336
O	-2.886302	0.846667	1.219709
O	-4.726470	1.602406	-0.721475
H	-4.265298	2.448209	-0.710115
I	0.541942	-0.303100	2.133843
O	-0.074184	-0.038566	0.418177
O	0.963028	1.373690	2.529059
O	-1.192283	-0.434231	2.896919
H	-1.854027	0.034808	2.326807
I	-0.660303	-1.986030	-0.687428
O	-2.342203	-1.802868	0.018311
O	0.190433	-2.740097	0.689257
O	-1.038273	-3.657807	-1.587876
H	-1.115391	-4.362953	-0.934575
I	3.194646	-0.431222	-0.699633
O	1.877614	-1.220324	-1.602946
O	2.720539	-0.554880	1.038129
O	4.401503	-1.948753	-0.648538
H	3.942502	-2.735450	-0.331317
I	0.750630	2.626284	-0.328809
O	2.207581	1.668768	-0.859840
O	1.218012	4.271393	-0.748496

O	-0.398735	2.283185	-1.797487
H	-1.087197	1.589417	-1.607616

(HIO ₃) ₆	X	Y	Z
I	2.280836	-0.275371	-2.188165
O	2.971955	-0.872037	-0.659824
O	0.760806	0.594918	-1.731637
O	3.332637	1.301417	-2.441340
H	2.951061	2.041162	-1.910397
I	0.641314	2.418481	-0.008352
O	-0.860818	3.000444	-0.864430
O	1.968343	3.166219	-0.937650
O	0.624309	3.776946	1.362662
H	1.194209	4.494499	1.058185
I	-2.789038	1.806879	-0.295319
O	-1.770938	1.317051	1.150570
O	-2.420066	0.654625	-1.591761
O	-4.394732	0.969560	0.361505
H	-4.165350	0.037867	0.546566
I	-1.458966	-1.032130	1.863806
O	-0.103187	-0.942134	0.638226
O	-2.876132	-1.326716	0.810706
O	-1.179524	-2.871406	2.294645
H	-1.206349	-3.347893	1.439473
I	-0.919657	-2.076491	-1.566663
O	-1.028149	-3.525209	-0.536283
O	0.778497	-2.174689	-2.188434
O	-1.772357	-2.849054	-3.116081
H	-1.667107	-3.808114	-3.074601

I	2.117361	-0.752483	2.044795
O	0.802444	-0.762562	3.268164
O	2.302812	0.984865	1.693578
O	3.617706	-0.937097	3.244489
H	3.656686	-0.169501	3.828595

Table S3 The ratio of the collision frequencies between the clusters and monomer molecule at the concentration C to the total evaporation frequencies of clusters ($\beta \cdot C / \Sigma \gamma$) of $(\text{HIO}_2)_{2-6}$ clusters and $(\text{HIO}_3)_{2-6}$ clusters at the RI-CC2/aug-cc-pVTZ (for O, H) + aug-cc-pVTZ-PP with ECP28MDF (for I) // ω B97X-D/6-311++G(3df,3pd) (for O, H) + aug-cc-pVTZ-PP with ECP28MDF (for I) level of theory at 268.15, 288.15 and 298.15 K and $P = 1$ atm. $C_1 = 2 \times 10^6$ molecules cm^{-3} for $(\text{HIO}_2)_{2-6}$ clusters, $C_2 = 1 \times 10^8$ molecules cm^{-3} for $(\text{HIO}_3)_{2-6}$ clusters.

Cluster	$\beta \cdot C_1 / \Sigma \gamma$ (268.15 K)	$\beta \cdot C_1 / \Sigma \gamma$ (288.15 K)	$\beta \cdot C_1 / \Sigma \gamma$ (298.15 K)
$(\text{HIO}_2)_2$	7.3×10^1	1.9×10^0	3.6×10^{-1}
$(\text{HIO}_2)_3$	3.9×10^4	5.1×10^2	8.0×10^1
$(\text{HIO}_2)_4$	2.8×10^3	4.4×10^1	7.4×10^0
$(\text{HIO}_2)_5$	1.7×10^1	4.6×10^{-1}	9.1×10^{-2}
$(\text{HIO}_2)_6$	2.8×10^6	2.8×10^4	2.7×10^3
Cluster	$\beta \cdot C_2 / \Sigma \gamma$ (268.15 K)	$\beta \cdot C_2 / \Sigma \gamma$ (288.15 K)	$\beta \cdot C_2 / \Sigma \gamma$ (298.15 K)
$(\text{HIO}_3)_2$	5.5×10^{-5}	5.8×10^{-6}	2.0×10^{-6}
$(\text{HIO}_3)_3$	2.5×10^{-3}	1.7×10^{-4}	4.8×10^{-5}
$(\text{HIO}_3)_4$	2.0×10^5	2.6×10^3	4.4×10^2
$(\text{HIO}_3)_5$	2.7×10^3	6.6×10^1	1.3×10^1
$(\text{HIO}_3)_6$	2.0×10^5	3.6×10^3	5.1×10^2

Table S4 The bond lengths of HIO₃ molecule in this study and three different polymorphs (α -HIO₃, β -HIO₃, γ -HIO₃)²⁻⁴. The values are shown in Å.

Bond	This study	α -HIO ₃	β -HIO ₃	γ -HIO ₃
	1.772,	1.783,	1.786,	1.791,
I-O	1.773,	1.812,	1.814,	1.804,
	1.945	1.896	1.903	1.873
O-H	0.966	0.996	0.960	0.911

Table S5 The thermal contribution to Gibbs free energy of formation ($\Delta G_{\text{thermal}}$) for (HIO₂)₂ and (HIO₂)₃ clusters by harmonic approximation calculations ($\Delta G_{\text{t-harm}}$) and anharmonic calculations ($\Delta G_{\text{t-anharm}}$) at the ω B97X-D/6-311++G(3df,3pd) (for O, H) + aug-cc-pVTZ-PP with ECP28MDF (for I) level of theory.

	$\Delta G_{\text{t-harm}}$ (hartree)	$\Delta G_{\text{t-anharm}}$ (hartree)	$ \Delta G_{\text{t-anharm}} - \Delta G_{\text{t-harm}} $ (kcal mol ⁻¹)
(HIO ₂) ₂	0.021393	0.021378	0.0094
(HIO ₂) ₃	0.043815	0.043827	0.0075

Section S5. References

1. H. Rong, J. Liu, Y. Zhang, L. Du, X. Zhang and Z. Li, *Chemosphere*, 2020, **253**, 126743.
2. K. Stahl and M. Szafranski, *Acta Chemica Scandinavica*, 1992, **46**, 1146-1148.
3. D. K. Smith, D. K. Unruh and M. L. Pantoya, *Advances in Materials Physics and Chemistry*, 2018, **8**, 246-256.
4. A. Fischer and M. Lindsjö, *Zeitschrift für anorganische und allgemeine Chemie*, 2005, **631**, 1574-1576.
5. A. K. Rappé, C. J. Casewit, K. S. Colwell, W. A. Goddard and W. M. Skiff, *Journal of the American Chemical Society*, 1992, **114**, 10024-10035.
6. J. Zhang and M. Dolg, *Physical Chemistry Chemical Physics*, 2015, **17**, 24173-24181.
7. J. Zhang and M. Dolg, *Physical Chemistry Chemical Physics*, 2016, **18**, 3003–3010.

8. M. J. McGrath, T. Olenius, I. K. Ortega, V. Loukonen, P. Paasonen, T. Kurten, M. Kulmala and H. Vehkamäki, *Atmospheric Chemistry and Physics*, 2012, **12**, 2345-2355.